Tellus (1999), 51A, 979–989
Printed in UK. All rights reserved

TELLUS
ISSN 0280–6495

Stability properties of a barotropic surface-water jet observed in the Denmark Strait

By TIM FRISTEDT[1]*, RIIKKA HIETALA[2] and PETER LUNDBERG[1], [1]*Department of Meteorology/Physical Oceanography, Stockholm University, 106 91 Stockholm, Sweden;* [2]*Finnish Institute of Marine Research, PO Box 33, FIN-00931 Helsinki, Finland*

(Manuscript received 29 August 1998; in final form 15 June 1999)

ABSTRACT

Observational data from a transect of the Denmark Strait have shown a rapid (1 m/s) southward-flowing barotropic surface jet. A linear stability analysis of the jet suggests that it may be unstable with respect to wavelike perturbations. The most unstable wave proved to be sinuous, i.e., meandering, with a growth rate of around 19 h (in terms of an *e*-folding time), a phase velocity of approximately 25 cm/s and wavelengths of around 40 km. Associated hydrographic data indicate that the local mixing of the surface waters predominantly is isopycnic. A possible explanation of this observed water-mass distribution could be that the jet initiated cross-channel water transports as the meandering instabilities grew with time. It must, however, be emphasised that since the stability properties of the jet are mainly locally determined, an overall description of the mixing processes in the area cannot be accomplished without invoking the along-stream variations of the flow.

1. Introduction

The Denmark Strait region between Iceland and Greenland (cf. the map in Fig. 1) has long been the object of scientific inquiry, since it constitutes an important choke point for the circulation of surface as well as subsurface water masses. Perhaps most interest has been devoted towards its controlling effects on the cold deep-water flow from the Greenland, Iceland and Norwegian seas, cf. Ross (1978); Smith (1976); Whitehead (1989). It must, however, also be noted that a very intense surface circulation occurs in the area with the cold East Greenland current transporting ice and low-saline cold water southwards, whereas the North Icelandic current on the easterly side of the passage carries warm and high-saline surface water of North Atlantic origin towards the Icelandic Sea. (This general situation was most recently summarised by Mauritzen (1996), who advanced an alternative circulation scheme for the Norwegian and Greenland Seas underlining the importance of Denmark Strait as a choke point for upper and intermediate water masses.) The thermohaline contrasts encountered in the area may lead to a rather complex hydrography, as can be appreciated from the composite TS-diagram in Fig. 2 representing a series of CTD stations worked across the passage on 30 August 1993. Here all the various water masses known to occur in the region are visible: Atlantic Water, Polar Water, Icelandic Sea Deep Water, and finally two water masses formed by mixing well north of the Denmark Strait (cf. Strass et al., 1993), viz. Polar Intermediate Water and Arctic Intermediate Water.

Since the Denmark Strait is more or less ice-covered during a considerable part of the year, it has not been subjected to as much experimental

* Corresponding author.
e-mail: tim@misu.su.se

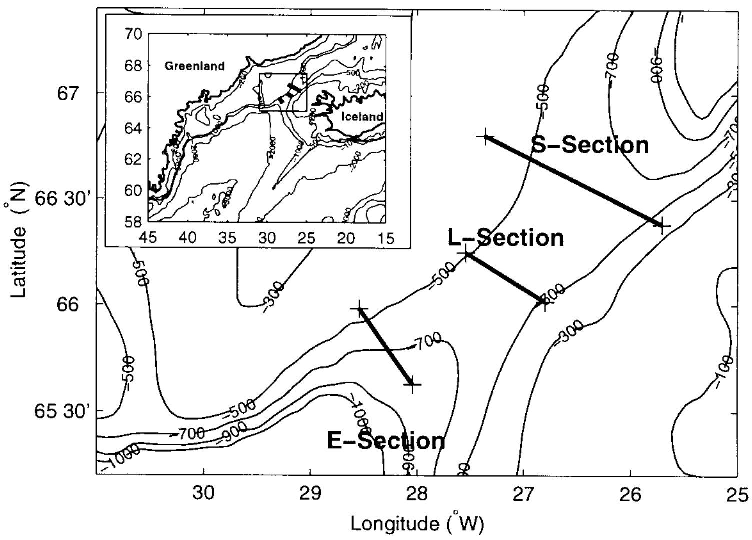

Fig. 1. Map showing the Denmark Strait and the location of the 3 sections E, L, and S, which were surveyed during the cruise.

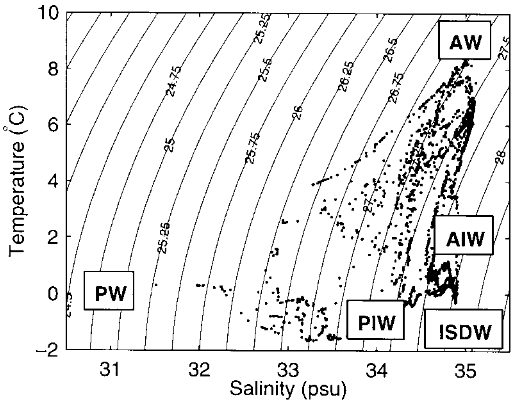

Fig. 2. TS-diagram summarising the hydrographic observations from the L-section on 30 August 1993. The 5 principal water masses are marked as AW = Atlantic Water, ISDW = Icelandic Sea Deep Water, PW = Polar Water, PIW = Polar Intermediate Water, AIW = Arctic Intermediate Water.

inquiry as many other oceanic choke points. In order to somewhat remedy this situation the Finnish Institute of Marine Research organised a cruise onboard the R/V Aranda to the area in August/September 1993 as a part of the Nordic-WOCE collaboration between Denmark, the Faroe Islands, Finland, Iceland, Norway and Sweden. The primary aim of this expedition was to observe the deep-water flux across the sill proper (viz. the Latrabjarg section shown as L in Fig. 1), but it was also recognised that the surface waters showed features of considerable interest, among them the barotropic jet which forms the topic of the present study.

In Section 2, a phenomenological description of the observed jet is given, whereafter a stability discussion is undertaken which indicates that this surface jet may be unstable. Section 5 is devoted to examining a set of hydrographic sections with possible bearing on the instability process. The study is concluded by a brief summary of the overall results, as well as a discussion of their relationship to previous investigations.

2 Observational results

The Denmark Strait transect to be focused upon was worked along the Latrabjarg section (cf. Fig. 1) on 30 August 1993. Hydrographic stations were taken at approximately every 4 nautical miles, accompanied by 150-kHz ADCP observations which, due to the moderate depths encountered in the area, were performed with the instrument set in the bottom-tracking mode and with a bin size of 8 m. As the vessel hove to, significant ADCP absolute velocities were

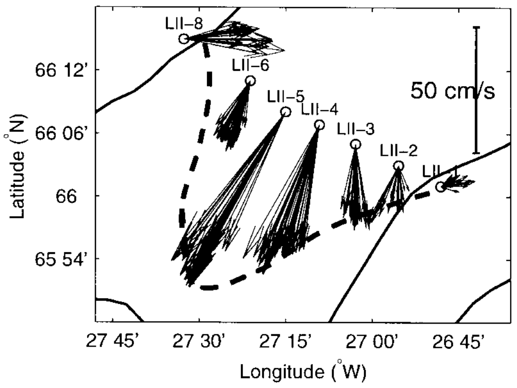

Fig. 3. ADCP velocity vectors superimposed on the geographical background for the L-section worked on 30 August 1993. For the seven stations the current vectors show the 30-min average for each depth bin down to approximately 350 m.

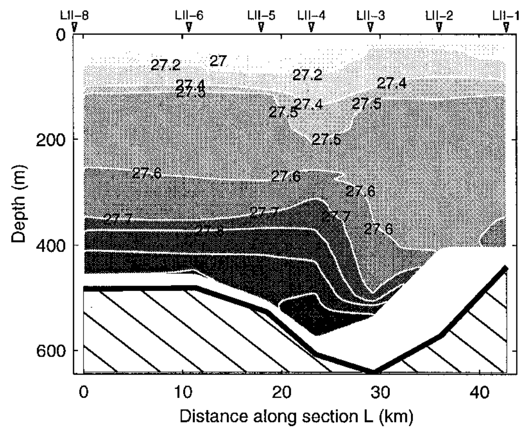

Fig. 4. Observed density distribution of the LII section surveyed on 30 August 1993 with the isopycnals labelled in σ-units.

obtained down to depths of around 350 m by averaging data from each bin over 30-min intervals. In Fig. 3 these observations are summarised in the form of a stick diagram (one current vector for each bin) superimposed on the topography. This graph demonstrates that not only does the flow take place at almost right angles to the transect, but also that the velocity vectors are practically independent of depth. (The deviations of velocity direction and magnitude over each vertical are of so small a magnitude that they quite likely may be attributed to measuring noise.)

Subject to the evident limitation that the present data set only encompasses one "snap-shot" of a single section, the overall impression from Fig. 3 is that we are dealing with a jet-like structure, orientated in the along-channel direction and displaying considerable vertical homogeneity. By decomposing the ADCP observations into along and cross-channel components, it is recognised that the latter velocity is very weak and directed towards the east. This motion is of sufficiently small average magnitude (~ 10 cm/s) to justify the assumption that the observed flow structure essentially may be characterised as an along-channel jet.

In Fig. 4, the results from the concurrent hydrographic survey are summarised in the form of the density distribution across the section. A noteworthy feature of the hydrography was that no pure Polar Water originating from the East Greenland current was observed on the section. However, the southbound Denmark Strait Overflow Water (DSOW) is clearly visible adjacent to the bottom primarily on the western side of the passage. This transport is composed of more-or-less pure deep water from the Iceland Sea ($\sigma_t > 28$), as well as Polar and Arctic intermediate water masses of somewhat lower densities. Note that the "pycnocline" at around $\sigma_t = 27.75$ (separating the well-defined overflow from the surface water masses) is located somewhat below the practical range of the ADCP (which was approximately 350 m). Thus the acoustical current observations only did justice to the motion of a surface water mass composed of a mixture of Atlantic and Polar Water. In this upper water mass, an anomalous density feature is visible at a depth of around 200 m in the region of station LII-4. This anomaly could be traced in the ADCP observations of the cross-channel velocity field, but it did not make a pronounced impact on the measured along-channel flow. A geostrophic velocity estimate (using the sea-surface as a reference level) yielded an upper bound of the associated baroclinic velocity anomaly of around 30 cm/s. This feature, which in many ways conforms to the concept of an "empty lens" (cf. Schultz-Tokos and Rossby, 1991), cannot a priori be neglected as a dynamical factor. A closer examination of the baroclinic features of the flow will be undertaken in connection with the forthcoming vorticity estimates. Finally it must be noted that tidal currents are of minor importance for the velocity field presently under consideration, since previous observations from the area show that these are of the magnitude 10 cm/s, cf. Mortensen et al. (1995); Uotila et al. (1997).

3. Potential vorticity considerations

In order to analyse the dynamics of the flow, the concept of a 2-dimensional barotropic jet has been adopted to characterise the observed velocity field (cf. Fig. 3), and consequently the along-channel variations of the flow will be neglected. Following Kuo's (1949) extension of the Rayleigh inflection-point theorem, it proves necessary to examine the cross-channel gradient of the potential vorticity so as to draw some conclusions about the stability of the flow. There are, however, two features of the available data material which further complicate the evaluation of the potential vorticity. *Pro primo*, the velocity measurements do not extend all the way down to the bottom, and, *pro secundo*, the water column is stratified. The uncertainties which the limited range of the ADCP gives rise to are primarily associated with the above-noted presence of Denmark Strait Overflow Water. Since it is known from previous studies, e.g., Worthington (1969); Stein (1988), that the velocity of this overflow generally has a magnitude in the range 50–100 cm/s there is no immediate reason to assume that the presence of the deep-water overflow will violate the simplified picture that we are dealing with a barotropic jet extending all the way down to the bottom.

The moderate density stratification visible in Fig. 4 could conceivably also be of importance for the distribution of vorticity q. The combined effects of density and velocity deviations from ideal homogeneous conditions may, following Pedlosky (1987), be estimated on the basis of the quasi-geostrophic form of the vorticity gradient:

$$\frac{\partial q}{\partial x} = \frac{\partial^2 v}{\partial x^2} - \frac{1}{\rho}\frac{\partial}{\partial z}\left\{\frac{f^2 \rho}{N^2}\frac{\partial v}{\partial z}\right\}. \tag{1}$$

Here, v is the horizontal along-channel velocity, ρ the density, g the acceleration of gravity, x and z the lateral and vertical co-ordinates, respectively, f denotes the Coriolis parameter, and $N^2 = -(g\rho)^{-1}\,\partial\rho/\partial z$ is the square of the Brunt-Väisala frequency. The 1st term on the r.h.s. of this equation corresponds to the horizontal shear, whereas the 2nd term describes the combined effect of stratification and vertical shear. An examination of the velocity and density distributions indicates that both the deep-water overflow and the "lens" are characterised by roughly the same scales, and hence these two anomalous features may be dealt with in a unified manner. On the basis of $\Delta v_x \sim 0.8$ m/s, $\Delta v_z \sim 0.2$ m/s, $\Delta\rho \sim 0.3$ kg/m^3, $\Delta x \sim 10$ km, $\Delta z \sim 100$ m (the vertical length scale over which the density changes $\Delta\rho$), it is recognised that the "stratification/vertical shear term" is at least one order of magnitude smaller than the "horizontal shear term". Since the latter term is dominant, the distribution of potential vorticity $P(x) = (\mathrm{d}v/\mathrm{d}x + f)/H$ across the jet has been calculated (cf. Fig. 5b) on the basis of the horizontal gradient (estimated from adjacent stations) of the depth-averaged along-channel velocity component and the depth of the fluid column H, both of these shown in Fig. 5a.

The relationship between the potential vorticity distribution in a barotropic jet and the overall stability properties of the flow was stated by Kuo (1949), who derived a necessary (but not sufficient) condition for instability which proved to be the rotating counter-part of Rayleigh's classical inflection-point theorem. Kuo showed that if the cross-jet distribution of potential vorticity possessed at least one extremum, it was possible for the jet to grow unstable. In the present case it has been shown in Fig. 5b that $P(x)$ possesses three extrema, and hence the possibility of amplifying

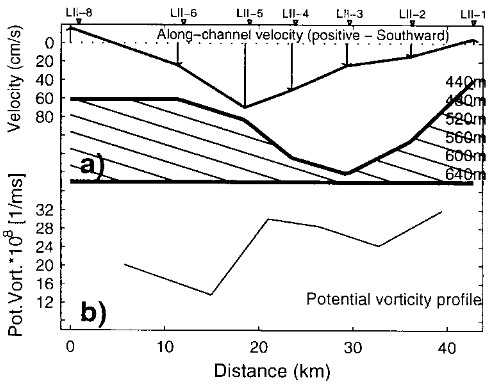

Fig. 5. (a) Velocity profile formed from the depth average of the along-channel component. (b) The simplified cross-channel potential vorticity distribution $P(x)$. The bottom profile is marked as the hatched area. In this graph the x-axis corresponds to the L-section with an orientation of 126° and the origin is located at station 8.

disturbances cannot be excluded. The important question whether the jet in fact was unstable will be dealt with in Section 4, which includes an analysis of the properties of growing perturbations.

4. Stability properties of the jet

In addition to demonstrating possible instability of the jet, the formal stability analysis may also be used to determine important characteristics of the most rapidly growing perturbations such as their wavelengths and growth rates. The technique to be applied here represents an application of a linear 2-dimensional theory based on conservation of potential vorticity. The method originates from the work of Ohshima (1987a), who examined the stability of a cosine-shaped barotropic jet over a rectilinear, sloping topography surrounded by areas of constant depth. In the present analysis the basic state is assumed to be an arbitrary velocity profile $v(x)$ in the form of a jet, flowing over a prescribed bottom topography $h(x)$. A perturbation field is expressed in terms of a transport streamfunction Ψ:

$$u^* = -\frac{1}{h}\frac{\partial \Psi}{\partial y}, \qquad v^* = \frac{1}{h}\frac{\partial \Psi}{\partial z}, \tag{2}$$

and the total solution $(u^*, v(x) + v^*)$ is inserted into the barotropic shallow-water equations. These are hereafter linearised with respect to the perturbative quantities, assumed to be wave-like, viz. $\Psi(x, y, t) = \Phi(x)\exp(i(\sigma t + ky)$. Here the amplitude solely is a function of the cross-channel co-ordinate x, k is the prescribed wave-number in the along-jet direction y, and the frequency is allowed to be complex ($\sigma = \sigma_r + i\sigma_i$), where the sign of σ_i determines whether the perturbation grows or decays as time goes by. Following Collings and Grimshaw (1980), this problem is resolved using a discretisation into segments over which both topography and basic-state velocity are treated as constants, hereby simplifying the perturbation equation. The governing equation is hereafter integrated across the discontinuities whereby matching conditions are obtained (physically equivalent to pressure continuity between the segments). The mass flux is also subjected to conditions of this type, requiring the amplitude $\Phi(x)$ to be continuous. The matching conditions for all segments (in addition to the natural boundary condition that the perturbations die out far from the jet) ultimately yield a set of linear algebraic equations, which can be reformulated as a characteristic-value problem with the reciprocal of the frequencies ($1/\sigma$) as the eigenvalues and the perturbation amplitude $\Phi(x)$ as the eigenvectors. This system is readily solved using matrix inversion, whereafter the unstable wave solutions are identified using the reciprocal eigenvalues with a non-zero imaginary part.

In the present case, the bathymetry and the observed velocity distribution of the jet were interpolated cubically on the basis of the zero-velocity endpoints (visible at 5 and 40 km along the x-axis in Fig. 5a), whereafter a discretisation into 30 constant segments was undertaken. (This resolution was adequate to fully resolve the unstable waves, as was demonstrated by a series of complementary experiments with 40- and 50-step discretisations.) The idealisation that the jet is surrounded by infinite areas of constant depth represents a simplification, not least due to the presence of coasts. The widths of the comparatively flat Greenland and Iceland shelves are, however, measured in hundreds of kilometres (compared to a lateral extent of the jet of only around 35 km), and hence it is assumed that the approximation is permissible. It may furthermore be demonstrated a posteriori that the stability properties of the jet primarily are locally determined and therefore only are weakly affected by the far-field boundary conditions. The numerical calculations ultimately yielded the eigenvalue-wavenumber relations shown in Fig. 6a,b, where $\sigma_r(k)$ and $\sigma_i(k)$ represent the fastest growing wave-like disturbance for each k. (The wavenumber k was taken to range between 0.1 to 8.0, with a resolution of $\Delta k = 0.1$.) The globally most rapidly growing wave-disturbance was found to be characterised by $\sigma_r = -0.27$, $\sigma_i = 0.11$ and $k = 5.1$. In dimensional form, this corresponds to an unstable wave with a growth rate (in terms of an e-folding time) of 19 h, a phase velocity of 25 cm/s and a wavelength of around 40 km (These dimensional quantities are based on the rotational timescale $1/f$ and a length scale taken to be the jet width equal to 35 km). The corresponding streamfunction is shown in Fig. 6c, from which it is recognised that this symmetric eigenfunction constitutes the gravest mode in the discrete spectrum of possible unstable solutions to

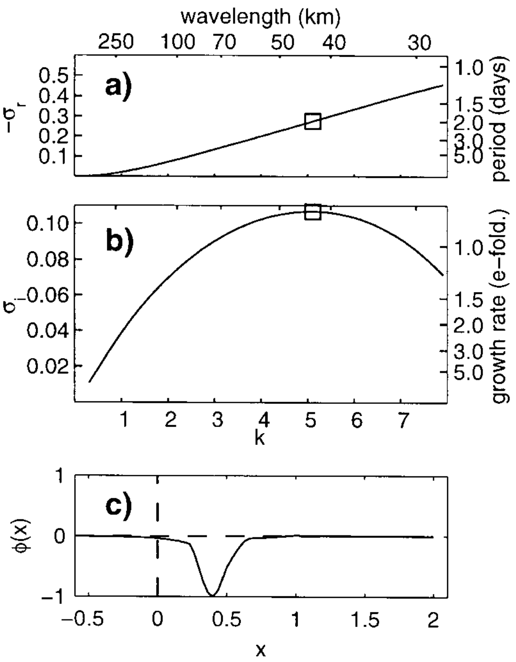

Fig. 6. (a,b) Dispersion relations for $\sigma_r(k)$ and $\sigma_i(k)$. (c) The streamfunction of the globally most unstable wave (indicated by a square in the graphs of $\sigma_r(k)$ and $\sigma_i(k)$).

the problem. In view of the definition of the streamfunction, this wave mode evidently represents instabilities of the meandering (or sinuous) type, cf. Pratt et al. (1995).

The analysis above was based on assuming that the jet had a fixed position relative the bottom topography. Since it, however, is difficult to envision a "free jet" constrained in this manner, a series of stability calculations for various transversal locations of the observed current field have also been undertaken. The dimensionless unit of measure a of the horizontal dislocation was taken to correspond to 35 km (i.e., the jet width), where a positive value of a denotes a shift towards Iceland. The bathymetric profile was extracted from a topographic data base and smoothed to the same degree as the topography used in the previous calculation. The same far-field boundary conditions for Φ as above were assumed, even though the dislocation of the basic jet was allowed to range from $a = -2$ to $a = +2$, corresponding to 70-km shifts towards Greenland and Iceland respectively.

The overall results from the calculations clearly illuminate the difference in stability properties of the jet for varying lateral positions in the strait. In Fig. 7a, the maximum growth rate (MGR), and its associated "most unstable wave-number" (k_{MGR}) are shown as functions of the dislocation parameter a. It is recognised that when $a < 0$, the maximum growth rate is characterised by an e-folding time of around 19 h, whereas for $a > 0$ it is of the order of 24 h. The associated wave-numbers of the fastest-growing perturbations are smaller when the jet is on the Greenland side ($k \approx 5$, viz. a wavelength of around 40 km) than when it is located towards Iceland, where $k \approx 7$ (corresponding to a wavelength of approximately 30 km). A comparison between the dispersion relations in Fig. 7b,c ($a < 0$) and Fig. 7e,f ($a > 0$), indicates that this discrepancy of the instability characteristics may be attributed to the fact that the "gravest unstable mode" (cf. Fig. 6) is not realised when the jet is located on the Iceland side of the passage. By examining the associated eigenfunctions in this region (cf. Fig. 7g), it is recognised that the predominating instabilities here are the 2nd and 3rd modes. Since the streamfunction is symmetric for $a < 0$, a meandering behaviour is expected in this region, whereas for the jet on the Iceland side of the passage, the 2nd unstable mode (characterised by one zero-crossing) predominates. This demonstrates that when $a > 0$, the instability is of the varicose type, cf. Pratt et al. (1995).

These differences in the evolution of a wavelike disturbance of the basic-state jet reflect 2 dynamical situations. When the southward-flowing jet is located on the Greenland side of the passage it is said to be prograde, viz. flowing in the direction of propagation of topographic Rossby waves and hence permitting these waves to extract energy from the basic-state flow field. Hence the meandering instability may be interpreted as modified topographic Rossby waves, a view consonant with the results obtained by Maslowski (1996) in his recent numerical study of the East Greenland Front at latitudes around 75°N. On the other hand, when the basic-state jet is located adjacent to the Icelandic shelf it may be classified as retrograde, i.e., flowing counter to the direction of propagation of the topographic waves. This situation apparently is conducive for direct energy transfer from the basic-state flow to "high wave-

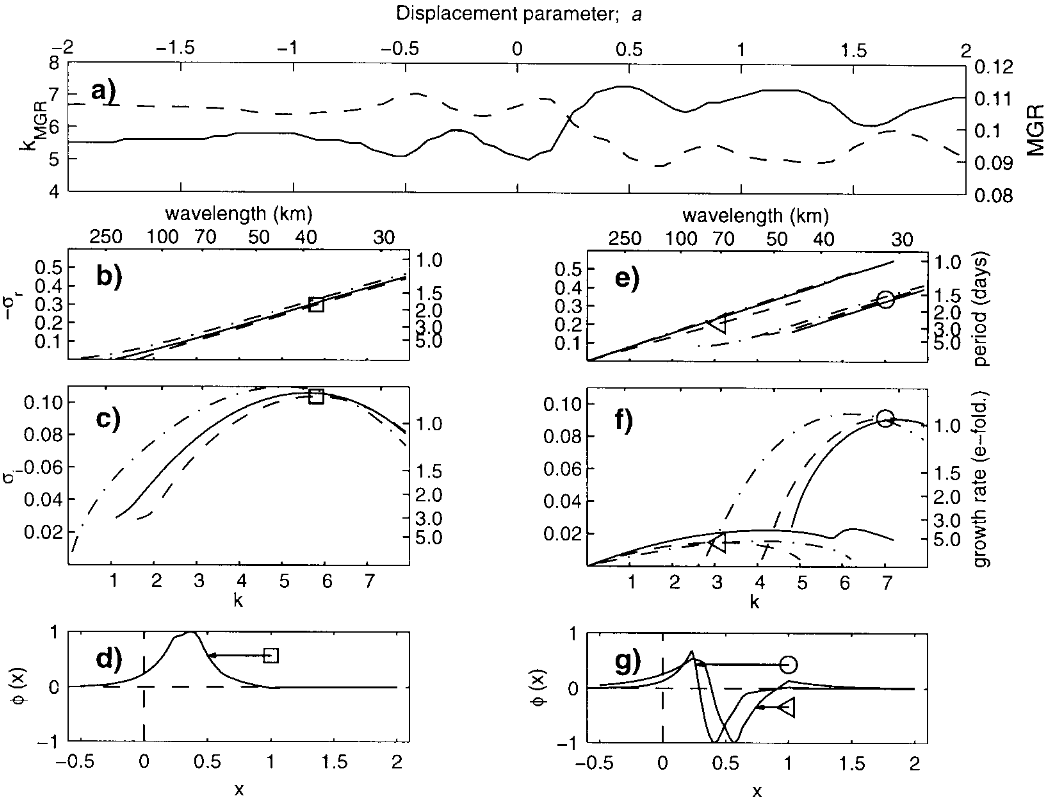

Fig. 7. Dispersion relations when the jet is moved relative the bottom topography. (a) The dashed line is the Maximum Growth Rate (MGR) and the full line shows the wavenumber of the corresponding wave, as functions of the parameter a, where $a = 1$ corresponds to a dislocation of one jet width 35 km towards Iceland and $a = -1$ one width towards Greenland. In (b) and (c) the dispersion relations for $a = \{-0.5, -1, -1.5\}$ = {dash-dotted, dashed, full} are shown and the rectangle indicates the globally most unstable wave for the case $a = -1$ with the corresponding streamfunction shown in (d). In (e) and (f) the dispersion relations for $a = \{0.5, 1, 1.5\}$ = {full, dashed, dash-dotted} are shown and the circle pertains to the most unstable wave for $a = 1$, which is the 2nd mode of unstable wave. The 3rd mode is indicated by a triangle also visible in (e) and (f). The streamfunctions of these two modes are shown in (g).

number" disturbances, leading to these perturbations demonstrating the most rapid growth rates.

This section pertaining to the more-or-less formal aspects of the eigenvalue analysis may be concluded by noting that an elegant solution to a closely related stability problem recently has been presented by Paldor and Ghil (1997).

5. Hydrographic cross-channel surveys

As recognised from the analysis of Section 4, there is a distinct possibility that the observed jet may have been unstable. Whether this in fact was the case and, perhaps even more important, if the jet represents a persistent feature of the Denmark Strait surface-water circulation remain vexing questions. These are difficult to answer, primarily due to lack of adequate field data, since most surveys in the area have focused on the deep-water overflow. As an attempt to cast some light over this problem, we will here try to draw some conclusions from the hydrographic data set from the region which was obtained during the R/V Aranda survey.

During the cruise a number of hydrographic sections were worked along the three transects denoted E, L, and S in the map of Fig. 1. Due to an exceptionally severe ice situation the research vessel could unfortunately not proceed as far up the Greenland shelf as would have been desirable, but nevertheless some interesting results emerged. The CTD-sections have been represented in the form of isotherm plots and are shown in Fig. 8. They demonstrate a rather unusual temperature structure at shallow and intermediate depths, viz. 50–400 m. (The same holds true for the salinities, but for the sake of brevity the forthcoming discussion will be conducted solely in terms of the temperatures.) The "normal case" expected in the area would be a frontal situation with warm, high-saline Atlantic waters on the Icelandic side of the strait and colder and fresher Polar waters in the East Greenland current on the western side of the passage. However, during the cruise reported here, a number of the temperature and salinity sections showed a situation where cold polar water was most abundant in the central part of the hydrographic sections, laterally enclosed by warmer waters as shown in Fig. 8. A TS-analysis showed that the warm water mass on the western side of the passage also must be of Atlantic origin (although note that its full extent westwards is unknown). One could visualise a coherent recircu-

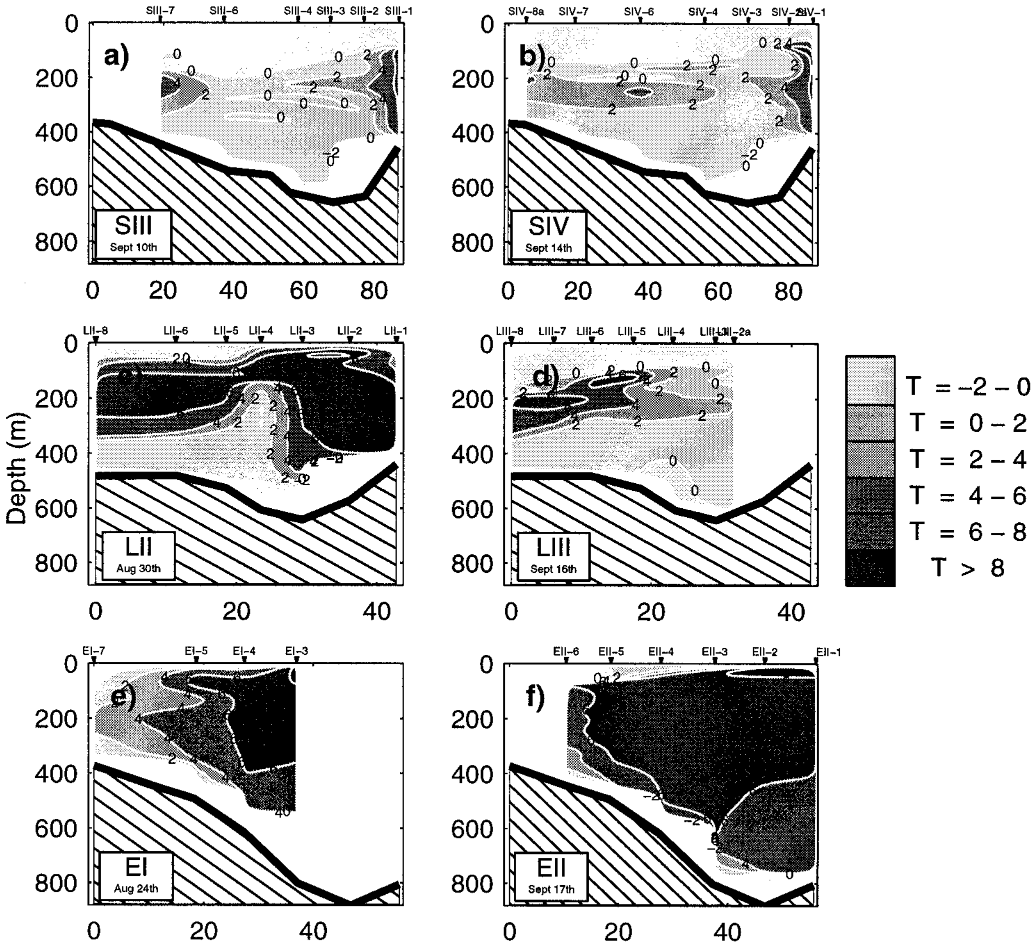

Fig. 8. Isotherm plots of some of the sections worked during the cruise in 1993. The sections are shaded according to the legend and consecutively numbered according to the order in which they were surveyed. The ordinates mark the horizontal location relative to each section and the abscissa marks the depth. (a) SIII-930910, (b) SIV-930914, (c) LII-930830, (d) LIII-930916, (e) EI-930824, (f) EII- 930917.

lation of Atlantic Water north of the sections shown in the map as being responsible for this TS-structure, but this does not appear very plausible in the light of previous oceanographic experiences from the area.

In Fig. 8 the two S-sections clearly show this feature of cold Polar Intermediate Water ($<0^{\circ}$C) bordered by warmer but more saline Atlantic Water (4–8°C). From these sections it is furthermore seen that a connecting tongue of warm Atlantic Water stretches across the strait at a depth of around 200 m. The L-sections, located at the sill, show similar features. In section LII, the Atlantic Water extends across the whole measured area and appears to be in the process of being "pinched off" by a water mass consisting mainly of Polar Intermediate Water. In section LIII, an isolated bolus of warm Atlantic Water is seen on the western side of the passage, which on the Icelandic side only contains cold water originating from north of the sill. For the sections south of the sill, section EII shows predominantly Atlantic Water in the whole section, whereas for section EI signs of isopycnal interleaving are clearly in evidence.

These sections (alternatively summarised in the form of TS-diagrams) suggest that the mixing is predominantly horizontal and that the coherent temperature structures are aligned with the isopycnals. (Similar filaments and more-or-less isolated "blobs" have previously been observed in the area by Stein (1988), who underlined the importance of horizontal exchange processes for the distribution of temperature and salinity.) This indicates that we are dealing with isopycnic mixing, singled out by Woods et al. (1986) as a significant process for the interaction between water masses in frontal areas, and suggested by Strass et al. (1993) as being important in the Iceland/Greenland Sea region adjacent to the East Greenland Current. Both of the latter studies emphasised the rôle of baroclinic processes in the modification of water masses. However, for the data set presently under consideration the meandering instability could provide a barotropic mechanism initiating horizontal water exchange. The growing perturbations would tend to move water in the cross-channel direction, a process which most likely would result in a temperature structure similar to that visible in the sections discussed above.

The precise amount of weight to be allotted to this "evidence" pointing in the direction of an unstable jet is of course debatable, particularly in the light of flow changes in the along-channel direction. Nevertheless it may be stated that the hydrographic structures visible in Fig. 8 conform to expectations associated with the consequences of a barotropically unstable meandering jet. The fact that the hydrographic observations were made over an extended period of time would (on the basis of the proposed instability mechanism) also tend to strengthen the belief that the jet was, at least during the period of the survey, a persistent feature of the surface water circulation.

Finally it may be worthwhile to point out that the horizontal mixing process outlined above has, on the basis of observations as well as numerical modelling, recently been reported by Gawarkiewicz and Plueddemann (1995) as being of critical importance along the Barents Sea polar front. A closely related mechanism, based on instabilities of topographic Rossby waves, has furthermore been suggested by Maslowski (1996) as a causative agent for the mixing of water masses along the East Greenland Front between 72°N and 77°N. Observations of the same type from the Soya warm current north of Japan have been reported by Ohshima (1987b), who explained them in terms of barotropic instability processes inducing cross-flow isopycnal transports. His conclusions were based on several observational data sets showing filaments and wave-like patterns extruding from a warm-water boundary current into an adjacent colder water mass. In a similar vein Paldor and Ghil (1997) recently suggested an analogous mixing mechanism for the Gulf Stream on the basis of a layered model.

6. Summary and conclusions

In the study presented here, various pieces of evidence have been assembled which indicate that the barotropic surface-water jet observed in the Denmark Strait may have been unstable. The most direct evidence was based on the CTD and ADCP observations at the sill obtained from N/O Aranda during the field experiment, mediated via stability considerations. (Due to the limited observational material available, this latter analysis was based on 2-dimensional formalism and thus did not encompass the possibility of convective instability, cf. Merkine (1977), which most certainly would change the down-stream character of the flow.) It has furthermore been shown that other hydrographic sections taken across the Denmark Strait also demonstrated a thermal structure indicative of cross-passage transports in the upper layer. This is an interesting fact which does not contradict the ideas advanced above concerning possible instability of the jet and its development.

A pronounced weakness of the present study is that it does not provide any information about the possible persistency of the jet. (The hydrographic results, as noted above, indicate that it may have been a persistent feature of the surface circulation during the period when the field survey was conducted.) With this essential *caveat* in mind, it may be permissible to conclude the study by indulging in some speculative considerations. As previously underlined, the dynamical process in the Denmark Strait region which has attracted most attention is the deep-water overflow, this due to its important implications for the global circulation. This phenomenon has primarily been investigated somewhat downstream of the sill proper, where the fully developed deep-water plume has been monitored, cf. Dickson et al. (1990); Dickson and Brown (1994); Ross (1978). A characteristic feature of the descending plume in this region has been a velocity fluctuation with a period of 1 to 2 days, cf. Aagaard and Malmberg (1978). This interesting and very striking property of the velocity field has been the object of considerable inquiry, cf. Smith (1976); Bruce (1995); Spall and Price (1998). These studies concerning the mechanisms underlying the observed periodicity of the flow have focused on the dynamics of the deep-water plume as it debouches down the slope into the North Atlantic proper. In view of the results discussed in the present study one could, however, permit oneself to hypothesise that the suggested instability of the barotropic surface-water jet could provide an alternative mechanism, based on regarding the jet as a causative agent subjecting the the deep-water flow to disturbances. The overflow would in this case be affected by a barotropic forcing with a characteristic period approximately equal to the one observed in the plume farther downstream. There is, however, reason to emphasise that this final notion, which represents a radical departure from previous ideas, cf. Smith (1976); Bruce (1995); Spall and Price (1998), must be regarded as extremely tentative. Evidently, much further inquiry in the field is necessary before anything more definite can be stated in this matter.

7. Acknowledgements

The work was supported by the Nordic Council of Ministers within its environmental research programme, the Finnish Institute of Marine Research, the Knut and Alice Wallenberg foundation, the Swedish Natural Science Research Council and the European Union under its VEINS programme.

REFERENCES

Aagaard, K. and Malmberg, S.-A. 1978. Low-frequency characteristics of the Denmark Strait overflow. *Int. Counc. for the Explor. of the Sea* **C:47**.

Bruce, J. G. 1995. Eddies southwest of the Denmark Strait. *Deep-Sea Res.* **42**, 13–29.

Collings, I. L. and Grimshaw, R. 1980. The effect of topography on the stability of a barotropic coastal current. *Dyn. Atmos. Oceans* **5**, 83–106.

Dickson, R. R. and Brown, J. 1994. The production of North Atlantic deep water: sources, rates and pathways. *J. Geophys. Res.* **99**, 12,319–12,341.

Dickson, R. R., Gmitrowicz, E. M. and Watson, A. J. 1990. Deep-water renewal in the northern North Atlantic. *Nature* **344**, 848–850.

Gawarkiewicz, G. and Plueddemann, A. J. 1995. Topographic control of thermohaline frontal structure in the Barents Sea Polar front on the south flank of Spitsbergen Bank. *J. Geophys. Res.* **100**, 4509–4524.

Kuo, H. L. 1949. Dynamic instability of two-dimensional non-divergent flow in a barotropic atmosphere. *J. Meteor.* **6**, 105–122.

Maslowski, W. 1996. Numerical simulations of topographic Rossby waves along the East Greenland front. *J. Geophys. Res.* **101**, 8775–8787.

Mauritzen, C. 1996. Production of dense overflow waters feeding the North Atlantic across the Greenland–Scotland ridge. Part 1: Evidence for a revised circulation scheme. *Deep-Sea Res.* **43**, 769–806.

Merkine, L.-O. 1977. Convective and absolute instability of baroclinic eddies. *Geophys. Astrophys. Fluid Dyn.* **9**, 129–157.

Mortensen, J., Briem, J., Buch, E. and Malmberg, S.-A.

1995. Western Iceland Project, Greenland Sea Project, moored current meter data, Greenland — Jan Mayen, Denmark Strait and Kolbeinsey Ridge, September 1990 to September 1991. *Hafrannsóknastofnun, Fjölrit* (Report of the Marine Research Institute of Iceland, Reykjavik) **41**, 173 pp.

Ohshima, K. I. 1987a. Stability of a barotropic jet on a sloping bottom. *J. Oceanogr. Soc. Japan* **43**, 49–60.

Ohshima, K. I. 1987b. On the stability of the Soya warm current. *J. Oceanogr. Soc. Japan* **43**, 61–67.

Paldor, N. and Ghil, M. 1997. Linear instability of a zonal jet on an f-plane. *J. Phys. Oceanogr.* **27**, 2361–2369.

Pedlosky, J. 1987. *Geophysical fluid dynamics*, 2nd edition. Springer-Verlag.

Pratt, L. J., Lozier, M. S. and Beliakova, N. 1995. Parcel trajectories in quasigeostrophic jets: neutral modes. *J. Phys. Oceanogr.* **25**, 1451–1466.

Ross, C. K. 1978. Overflow variability in Denmark Strait. *Int. Counc. for the Explor. of the Sea* **C:21**.

Schultz-Tokos, K. and Rossby, T. 1991. Kinematics and dynamics of a Mediterranean salt lens. *J. Phys. Oceanogr.* **21**, 879–892.

Smith, P. C. 1976. Baroclinic instability in the Denmark Strait overflow. *J. Phys. Oceanogr.* **6**, 355–371.

Spall, M. A. and Price, J. F. 1998. Mesoscale variability in the Denmark Strait: The PV outflow hypothesis. *J. Phys. Oceanogr.* **28**, 1598–1623.

Stein, M. 1988. Variability of water masses, currents and ice in Denmark Strait. *NAFO Sci. Coun. Studies* **12**, 71–84.

Strass, V. H., Fahrbach, E., Schauer, U. and Sellmann, L. 1993. Formation of Denmark Strait overflow water by mixing in the East Greenland Current. *J. Geophys. Res.* **98**, 6907–6919.

Uotila, J., Launiainen, J. and Vihma, T. 1997. An analysis buoy drift in the northern North Atlantic with detection of drogue loss events. *Atmosphere Oceans* **35**, 471–494.

Whitehead, J. A. 1989. Internal hydraulic control in rotating fluids. Applications to oceans. *Geophys. Astrophys. Fluid Dyn.* **48**, 169–192.

Woods, J. D., Onken, R. and Fischer, J. 1986. Thermohaline intrusions created isopycnically at oceanic fronts are inclined to isopycnals. *Nature* **322**, 446–449.

Worthington, L. V. 1969. An attempt to measure the volume transport of Norwegian Sea overflow water through the Denmark Strait. *Deep-Sea Res.* (suppl. **16**), 421–432.